Evidence That Hypothalamic Gliosis Is Related to Impaired Glucose Homeostasis in Adults With Obesity

Jennifer L. Rosenbaum,[1] Susan J. Melhorn,[2,3] Stefan Schoen,[4] Mary F. Webb,[2,3] Mary Rosalynn B. De Leon,[2,3] Madelaine Humphreys,[2,3] Kristina M. Utzschneider,[1,5] and Ellen A. Schur[2,3]

Diabetes Care 2022;45:416–424 | https://doi.org/10.2337/dc21-1535

OBJECTIVE

Preclinical research implicates hypothalamic glial cell responses in the pathogenesis of obesity and type 2 diabetes (T2D). In the current study we sought to translate such findings to humans by testing whether radiologic markers of gliosis in the mediobasal hypothalamus (MBH) were greater in individuals with obesity and impaired glucose homeostasis or T2D.

RESEARCH DESIGN AND METHODS

Using cross-sectional and prospective cohort study designs, we applied a validated quantitative MRI approach to assess gliosis in 67 adults with obesity and normal glucose tolerance, impaired glucose tolerance (IGT), or T2D. Assessments of glucose homeostasis were conducted via oral glucose tolerance tests (OGTT) and β-cell modeling.

RESULTS

We found significantly greater T2 relaxation times (a marker of gliosis by MRI), that were independent of adiposity, in the groups with IGT and T2D as compared with the group with normal glucose tolerance. Findings were present in the MBH, but not control regions. Moreover, positive linear associations were present in the MBH but not control regions between T2 relaxation time and glucose area under the curve during an OGTT, fasting glucose concentrations, hemoglobin A_{1c}, and visceral adipose tissue mass, whereas negative linear relationships were present in the MBH for markers of insulin sensitivity and β-cell function. In a prospective cohort study, greater MBH T2 relaxation times predicted declining insulin sensitivity over 1 year.

CONCLUSIONS

Findings support a role for hypothalamic gliosis in the progression of insulin resistance in obesity and thus T2D pathogenesis in humans.

The brain plays an increasingly recognized role in metabolic control, and therefore impairments in glucoregulatory action at the level of the brain might contribute to the pathophysiology of type 2 diabetes (T2D) (1,2). A growing literature derived from animal models reveals that inflammation in the hypothalamus promotes both obesity and abnormal glucose metabolism (3–6). Located in the mediobasal hypothalamus (MBH), the arcuate nucleus is primarily implicated in this pathophysiologic

[1]Division of Metabolism, Endocrinology and Nutrition, Department of Medicine, University of Washington, Seattle, WA
[2]Division of General Internal Medicine, Department of Medicine, University of Washington, Seattle, WA
[3]UW Medicine Diabetes Institute, University of Washington, Seattle, WA
[4]University of Washington School of Medicine, Seattle, WA
[5]Research and Development, Department of Veterans Affairs, Seattle, WA

Corresponding author: Ellen A. Schur, ellschur@uw.edu

Received 23 July 2021 and accepted 3 November 2021

This article contains supplementary material online at https://doi.org/10.2337/figshare.16941028.

process. It contains neuronal populations, including proopiomelanocortin cells, that are critical to energy and glucose homeostasis, in part because they transduce input from afferent signals, such as leptin and insulin (7), but also because they interact with local glial cells to modulate circulating glucose levels (8–10). In rodents, a high-fat diet rapidly triggers inflammation, neuronal injury, and a reactive gliosis in the arcuate nucleus (4,11,12). In addition, prolonged dietary insults have been found to reduce proopiomelanocortin cell numbers (4). The resulting disruption of arcuate nucleus signaling pathways might impair central nervous system (CNS) glucose regulation or promote increasing adiposity. Thus, hypothalamic gliosis might either directly or indirectly facilitate progression to type 2 diabetes.

MRI techniques documented the first evidence for hypothalamic gliosis in humans with obesity (4). These findings have since been replicated (13–15) and expanded to show evidence of hypothalamic gliosis in children with obesity (16,17) and postmortem specimens from adults with obesity (18). Additionally, subjects with metabolic syndrome and T2D also show evidence of hypothalamic inflammation and gliosis (15,19). Data are inconsistent though as to whether subclinical insulin resistance is related to hypothalamic gliosis. While in one study radiologic markers of MBH gliosis were positively associated with fasting insulin concentrations and HOMA of insulin resistance (14), investigators in a second study found no association (13). Both studies were limited by a cross-sectional approach, with only fasting measures examined. Moreover, visceral adiposity, with its concomitant elevated metabolic risk, appears to increase in direct proportion to the extent of MBH gliosis by MRI (17,20). Human studies of hypothalamic gliosis have yet to test relationships with impaired glucose tolerance (IGT) or β-cell responses, and prospective longitudinal data are not available for assessment of change over time in measures of glucose homeostasis.

In the current study we implemented a validated (12,14) quantitative MRI technique for the assessment of gliosis in the hypothalamus and applied this technique to establish the relationship of MBH gliosis with impaired glucose homeostasis in humans. In a cross-sectional approach, we first tested for increased evidence of gliosis within the MBH versus control brain regions among adults with obesity and IGT or T2D compared with those with normal glucose tolerance (NGT), as determined by an oral glucose tolerance test (OGTT). Second, using a prospective longitudinal cohort study approach limited to participants with obesity but not T2D, we tested whether greater radiologic evidence of MBH gliosis at baseline was a risk factor for deterioration in measures of glucose homeostasis and adiposity over 1 year of observational follow-up. Finally, we determined whether findings were independent of adiposity to assess whether hypothalamic gliosis and impaired glucose homeostasis could be directly related in humans as opposed to indirectly linked through adiposity.

RESEARCH DESIGN AND METHODS

Participants

A total of 69 individuals ages 25–60 years with obesity were recruited from the Seattle area with flyers, advertisements, mailed invitations, the UW Medicine Diabetes Institute Community of Volunteers Engaged in Research to End Diabetes (COVERED) Registry, and a diabetes registry maintained by the Veterans Affairs–based Diabetes Research Group. Exclusion criteria included a history of bariatric surgery, poorly controlled hypertension, coronary artery disease, type 1 diabetes, or other chronic disease. Participants with T2D needed to have a hemoglobin A_{1c} between 6.5 and 8.0%, be <10 years from diagnosis, and not take insulin. Additional exclusion criteria were use of weight loss medications or other medications known to impact body weight including glucagon-like peptide 1 agonists, dipeptidyl peptidase 4 inhibitors, and thiazolidinediones; use of metformin in a participant without diabetes; contraindications to MRI including weight >330 lb; current smoking; and heavy alcohol use. Per protocol, cross-sectional analyses included all participants with complete outcome data (*N* = 2 were excluded due to MRI artifact, resulting in *N* = 67). Longitudinal analyses included all participants without diabetes with complete MRI and OGTT data (*N* = 38) (Supplementary Fig. 1). Participants provided signed informed consent. Procedures were approved by the UW Institutional Review Board.

Study group assignment for participants without T2D was determined by plasma glucose values measured at the baseline visit: NGT (*N* = 29), 2-h glucose <140 mg/dL (7.8 mmol/L), and IGT (*N* = 21), 2-h glucose 140–200 mg/dL (7.8–11.1 mmol/L). The T2D group (*N* = 17) included three participants without a prior diagnosis who were reclassified due to 2-h glucose >200 mg/dL (11.1 mmol/L) or fasting glucose >126 mg/dL (7.0 mmol/L).

Study Procedures

Participants fasted overnight for ≥12 h and held diabetes medications for 72 h prior to study visits. Weight and height were measured in duplicate and the values were averaged. Only participants with a fasting blood glucose <200 mg/dL underwent OGTT. Body composition was measured in the fasted state with DEXA (iDXA; GE Healthcare, Madison, WI), and abdominal visceral adipose tissue (VAT) mass was determined with use of enCORE software (platform version 16.2; GE Healthcare). After 12 months, participants with NGT or IGT returned and study procedures, excluding MRI, were repeated.

OGTT

Blood draws were completed via intravenous catheter at −15, −5, 0, 10, 20, 30, 60, 90, and 120 min relative to the consumption (T = 0) of 75 g glucose solution over a maximum of 5 min. Glucose, insulin, and C-peptide from time points 0 through 120 min (*n* = 7) were used for area under the curve (AUC) calculations and β-cell modeling.

MRI Image Acquisition and Analysis

Methodology for the acquisition and analysis of MRI images has previously been published (14,16). In brief, MRI images were captured with an Achieva 3T scanner (version 5.1.7; Philips Medical Systems), a 32-channel head radiofrequency coil, and a quantitative multislice/multiecho T2-weighted sequence with 16 echoes (interecho spacing 10 ms). Images spanned from the optic chiasm to the mammillary bodies with a slice thickness of 2.0 mm (no gap). As previously implemented and validated (14,17,20), images were analyzed with OsiriX DICOM Viewer. The coronal slice

representing the rostral arcuate nucleus was identified as the slice immediately posterior to the visual split of the optic chiasm. With use of anatomical landmarks (21), the MBH—located adjacent to the 3rd ventricle and superior to the median eminence—and control regions in white matter and gray matter (putamen and amygdala) were identified (Fig. 1*D*). Regions of interest were placed bilaterally on high-resolution images and then transferred to T2 parametric maps, from which mean T2 relaxation time from individual regions of interest was extracted.

Laboratory Assays

Blood samples taken during the OGTT were collected in EDTA tubes and immediately placed on ice. Samples were centrifuged at 4°C, aliquoted, and stored at −80°C until assayed for glucose, insulin, and C-peptide. During the baseline visit, additional blood samples were collected in NaF tubes at times 0 and 120 min, analyzed immediately for glucose concentration via automated chemistry, and used to determine participant group assignment. ALT and AST were measured by automated chemistry. IL-6 was run on a one-step immunoenzymatic assay. C-reactive protein was measured with a high-sensitivity assay. Cholesterol was measured with cholesterol dehydrogenase assay, triglycerides were measured with microbial lipase, and HDL was measured with a two-reagent homogenous system, and LDL was calculated. Leptin, C-peptide, and insulin concentrations were measured with ELISA. Glucose concentrations during the OGTT were measured with a YSI analyzer system (YSI Inc., Yellow Springs, OH).

Calculations and β-Cell Modeling

Total AUC was calculated with the trapezoidal method; incremental AUC (iAUC) was calculated with the trapezoidal method accounting for each participant's time 0 value. The insulinogenic index was calculated as the ratio of early-phase iAUC insulin to glucose from 0 to 30 min ($iAUCins_{0–30}/iAUCglu_{0–30}$), the C-peptide index was calculated as ($iAUC\text{-}C\text{-}peptide_{0–30}/iAUCglu_{0–30}$, and the disposition

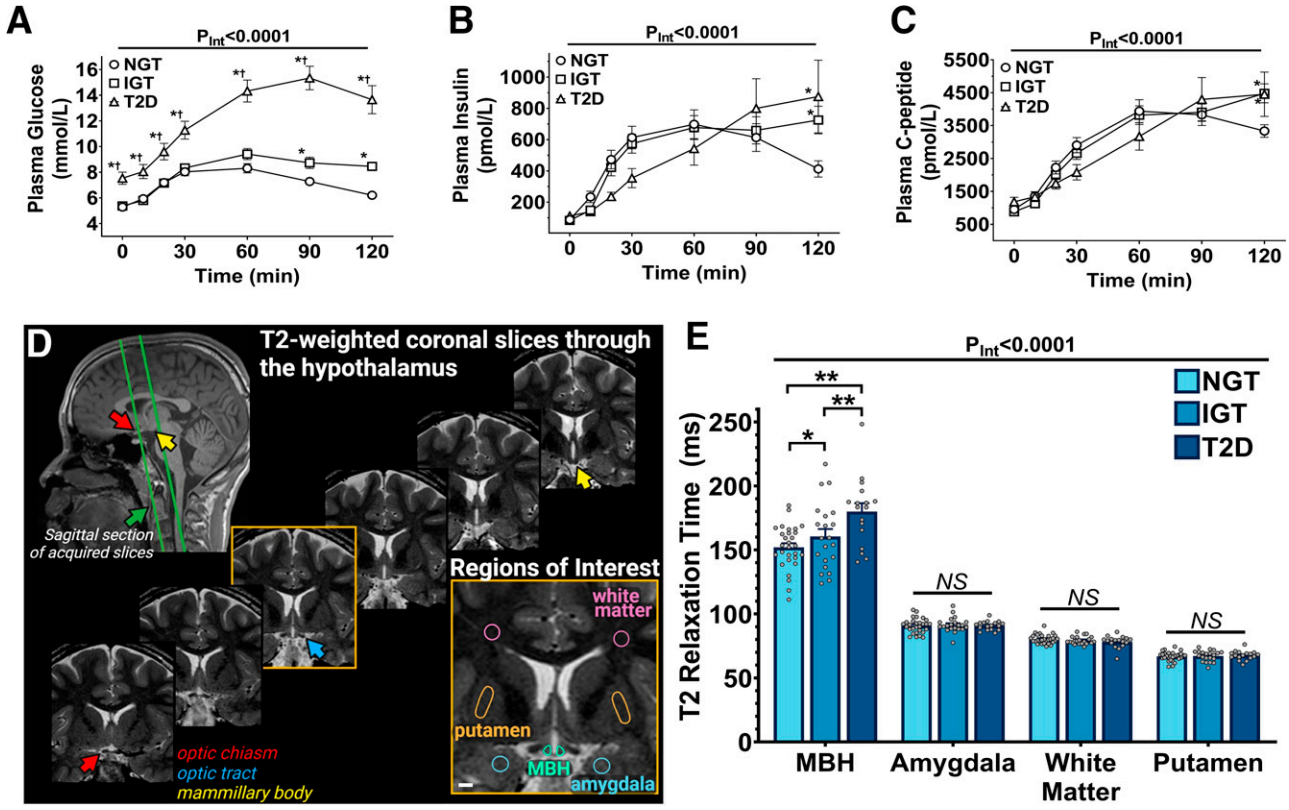

Figure 1—OGTT curves and MRI image acquisition and results by brain region of interest among participants with NGT, IGT, or T2D. *A*: The T2D group had significantly greater excursion of glucose throughout the OGTT compared with both IGT and NGT groups. The IGT group had significantly higher plasma glucose at 90 and 120 min compared with NGT. T2D and IGT groups had higher plasma insulin (*B*) and C-peptide (*C*) values 2 h after consumption of a glucose load compared with NGT. *D*: MRI image acquisition: upper left illustrates section of acquired coronal slices (between green lines) anteriorly from the optic chiasm extending posteriorly to the mammillary bodies in the sagittal plane (T1-weighted image). Serial images are T2-weighted coronal slices at echo time 110 ms with the slice of interest encompassing the MBH identified with gold border. Anatomic landmarks are identified with colored arrows (red, optic chiasm; blue, optic tract; yellow, mammillary body). Lower right shows representative T2-weighted coronal image with the MBH with control regions of interest identified. T2-weighted high-resolution images allow for visualization of anatomic landmarks and placement of regions of interest that are then transferred to a parametric map (not shown) from which T2 relaxation times are extracted. White scale bar represents 6 mm. *E*: A significant interaction indicated that group differences in T2 relaxation times varied by region of interest. Participants with IGT had longer mean MBH T2 relaxation time compared with participants with NGT, whereas participants with T2D had significantly longer mean MBH T2 relaxation time compared with both IGT and NGT groups. There were no group differences within gray (amygdala, putamen) or white matter control regions. *P* values by unadjusted generalized estimating equations with an interaction term (*A*–*C*) (group * time, $P_{interaction}$ [P_{int}]) or by linear mixed model with adjustment for age with an interaction term (*E*) (group * region, $P_{interaction}$), followed by formal post hoc testing for group differences. In *A*–*C*, $^*P < 0.01$ vs. NGT, $^\dagger P < 0.05$ vs. IGT; in *E*, $^*P = 0.008$, $^{**}P < 0.0001$. *N* = 29 (NGT), *N* = 21 (IGT), *N* = 17 (T2D). Missing data include *N* = 2 T2D in *A*–*C*.

index was calculated as follows: insulinogenic index * (1 / fasting insulin). We estimated β-cell glucose sensitivity by modeling glucose and C-peptide data. The model, in part, describes the relationship between insulin secretion (expressed in pmol · min^{-1} · m^{-2}) and glucose concentration (22,23), with the slope of the dose-response function relating these variables referred to as β-cell glucose sensitivity. The model parameters were estimated from glucose and C-peptide concentrations (with use of C-peptide deconvolution [24]) as previously described (22). A measure of insulin sensitivity (oral glucose insulin sensitivity [OGIS]) was obtained in accordance with prior work (25) using glucose and insulin data from the OGTT.

Statistical Analysis

Data are means ± SD unless otherwise indicated. Group differences for descriptive variables were assessed with χ^2 test (categorical variables), one-way ANOVA followed by Bonferroni-corrected posttest as appropriate (normally distributed), and Kruskal-Wallis rank test followed by Wilcoxon-Mann-Whitney test as appropriate (nonnormally distributed). A linear mixed model with restricted maximum likelihood estimation and an interaction term tested group-by-region differences for mean T2 relaxation time, followed by formal post hoc analyses when a significant interaction was present. Inferential analyses were adjusted for age unless otherwise noted. Generalized estimating equations models were used to assess the time course of plasma measures during the OGTT, included an interaction term for group by time, and were followed by group comparisons with formal posttests given all interaction terms were significant. Generalized estimating equations models tested associations between predictors and outcome of T2 relaxation time (including all brain regions) and included an interaction term (predictor * region) followed by posttests of linear associations within the MBH. Planned subgroup analyses were completed with the T2D group excluded. All statistics were completed in STATA (version 16), and graphing was completed in GraphPad Prism (version 8.4.3).

RESULTS

Participant Characteristics

Mean ± SD age was 48 ± 11 years, and 72% of participants were female. Mean BMI at study entry was 36 ± 4 kg/m^2. The mean duration of diabetes in the T2D group was 4.4 ± 3.4 years (range 0–10) and mean hemoglobin A_{1c} was 6.6 ± 0.7%. NGT, IGT, and T2D groups were well balanced by sex, race, and ethnicity and did not differ in liver function tests, plasma inflammatory markers, cholesterol levels, fasting leptin concentrations, or health behaviors around weight management and obesity (Table 1). The T2D group was significantly older, had higher fasting plasma triglycerides, and tended toward higher blood pressures. Adiposity and body composition as assessed based on mean BMI, % body fat, % lean mass, and VAT (g) did not differ between the groups.

As expected, the T2D group had significantly higher mean fasting plasma glucose, worse glucose tolerance, reduced β-cell function by disposition index and glucose sensitivity measures, and lower insulin sensitivity by OGIS compared with the NGT and IGT groups (Supplementary Table 1). The IGT group had higher mean plasma glucose concentrations 90 and 120 min post oral glucose load than the NGT group (Fig. 1*A*). Plasma insulin and C-peptide concentrations remained significantly elevated 120 min post–glucose load in both the IGT and T2D groups as compared with the NGT group (Fig. 1*B* and *C*). The IGT and NGT groups did not significantly differ in measures of β-cell function or insulin sensitivity (Supplementary Table 1).

Group Differences in Mean Bilateral T2 Relaxation Time

We tested whether groups differed in the MBH versus control regions by including a group * region interaction term in a linear mixed model adjusted for age, with a highly significant result (Fig. 1*E*). Bonferroni-corrected comparisons confirmed that age-adjusted bilateral mean MBH T2 relaxation times were significantly longer in the T2D as compared with the IGT and NGT groups and the IGT as compared with the NGT group (Fig. 1*E*). The significant group * region interaction ($\chi^2(6) = 65.4$, $P_{interaction} < 0.0001$) and group differences within the MBH persisted in a model with adjustment for sex and percentage of total body fat in addition to age (NGT vs. IGT, $P = 0.009$; NGT vs. T2D and IGT vs. T2D, $P < 0.0001$). The possibility of lateralized effects was interrogated using a model that included a main effect for side (right vs. left); no lateralization was found ($\chi^2(1) = 0.06$, $P = 0.81$).

Cross-sectional Associations of Measures of Glucose Homeostasis and Adiposity With T2 Relaxation Time

Among all participants, fasting plasma glucose concentrations and hemoglobin A_{1c} were positively associated with T2 relaxation time in the MBH but not in control regions (Fig. 2*A* and *B*), as was plasma glucose 2-h post–glucose load (β = 2.78 ms, $P < 0.0001$). Moreover, glucose tolerance as assessed by glucose iAUC was also positively related to longer MBH T2 relaxation times (Fig. 2*C*). Disposition index, glucose sensitivity, and insulin sensitivity as assessed by the OGIS index were all negatively related to T2 relaxation time in the MBH but not in control regions (Fig. 2*D*–*F* and Supplementary Table 2). In contrast, variation in total-body adiposity among adults with obesity was unrelated to MBH or control region T2 relaxation times (Fig. 2*G*). However, VAT deposition was positively associated with MBH, but not control region, T2 relaxation time (Fig. 2*H*).

Subgroup analyses were performed among participants without diabetes (Supplementary Table 2) and revealed significant positive relationships of MBH T2 relaxation time with hemoglobin A_{1c} and glucose iAUC. In addition, disposition index also remained significantly and negatively associated, whereas there was no longer an association with glucose sensitivity, and relationships with fasting glucose, OGIS, and VAT (β = −0.05 ms, $P = 0.07$) were attenuated to trends ($P \leq 0.1$).

Prospective Association of Baseline T2 Relaxation Time With Changes in Measures of Glucose Homeostasis and Adiposity Over 1 Year in Participants Without Diabetes

The average duration between baseline and 12-month follow-up assessments for the 38 participants with obesity and no diabetes was 12.5 months (SD =

Table 1—Participant characteristics with stratification by group

	NGT (*N* = 29)	IGT (*N* = 21)	T2D (*N* = 17)	Statistic	*P*
Female sex, %	76	67	71	$\chi^2(2) = 0.52$	0.77
Race, % White	82	67	59	$\chi^2(2) = 3.40$	0.18
Ethnicity, % non-Hispanic	93	95	88	$\chi^2(2) = 0.69$	0.71
Vitals, anthropometrics					
Age, years	45 ± 12	46 ± 11	54 ± 8*†	$\chi^2(2) = 8.71$	**0.02**
Heart rate, bpm	69 ± 11	68 ± 14	76 ± 10	$F(2,66) = 2.20$	0.12
Systolic blood pressure, mmHg	123 ± 11	122 ± 14	131 ± 14	$F(2,66) = 2.77$	0.07
Diastolic blood pressure, mmHg	79 ± 9	76 ± 12	83 ± 8	$F(2,66) = 2.66$	0.08
Weight, kg	105 ± 13	98 ± 11	104 ± 18	$F(2,66) = 2.40$	0.10
Waist, cm	120 ± 12	113 ± 9	118 ± 13	$F(2,66) = 2.24$	0.12
BMI, kg/m^2	37 ± 4.7	35 ± 3.1	37 ± 4.1	$F(2,66) = 1.72$	0.16
Fat, %	45 ± 7.9	45 ± 6.0	45 ± 7.3	$F(2,66) = 0.01$	0.99
Lean, %	55 ± 7.9	55 ± 6.0	55 ± 7.3	$F(2,66) = 0.01$	0.99
VAT, g	1,822 ± 936	1,601 ± 841	2,178 ± 1,147	$\chi^2(2) = 3.26$	0.20
Laboratories and plasma measures					
AST, units/L	21 ± 9.3	21 ± 7.6	23.2 ± 6.6	$\chi^2(2) = 2.74$	0.25
ALT, units/L	22 ± 12	23 ± 12	29 ± 15	$\chi^2(2) = 2.96$	0.23
IL-6, pg/mL	4.04 ± 2.88	3.90 ± 2.79	5.79 ± 6.71	$\chi^2(2) = 1.15$	0.56
C-reactive protein, nmol/L	40.1 ± 37.2	43.7 ± 40.0	62.6 ± 48.2	$\chi^2(2) = 3.11$	0.21
Cholesterol (total), mmol/L	4.57 ± 0.80	4.41 ± 0.69	4.46 ± 1.09	$F(2,66) = 0.40$	0.68
HDL, mmol/L	1.23 ± 0.24	1.25 ± 0.35	1.13 ± 0.27	$F(2,66) = 0.94$	0.94
LDL, mmol/L	2.83 ± 0.75	2.89 ± 0.55	2.50 ± 0.83	$F(2,63) = 1.38$	0.26
Triglycerides, mmol/L	1.30 ± 0.65	1.47 ± 0.72	3.02 ± 2.86*	$\chi^2(2) = 7.75$	**0.02**
Leptin, nmol/L	2.55 ± 2.01	2.33 ± 1.55	2.36 ± 1.69	$\chi^2(2) = 0.23$	0.99
Behavioral measures					
Weight reduced, % from maximum‡	5.7 ± 5.2	6.8 ± 5.9	8.3 ± 5.3	$\chi^2(2) = 3.84$	0.15
Currently attempting to lose weight, % yes	74	80	71	$\chi^2(2) = 0.46$	0.80
Activity (moderate + vigorous), MET min/week§	720 (240–1,440)	640 (210–1,760)	660 (0–1,280)	$\chi^2(2) = 0.92$	0.63
Cognitive restraint‖	13.0 ± 3.0	14.5 ± 2.5	13.8 ± 2.3	$F(2,66) = 2.03$	0.14
Uncontrolled eating‖	19.1 ± 4.7	18.3 ± 3.3	20.4 ± 5.0	$F(2,66) = 1.00$	0.37
Emotional eating‖	8.2 ± 2.6	8.0 ± 2.2	8.1 ± 2.2	$F(2,66) = 0.05$	0.95

Data are means ± SD or median (interquartile range) unless otherwise reported. Participants were assigned to groups at baseline based on medical history, laboratory studies, and OGTT results. Groups were compared by χ^2 test for categorical variables and one-way ANOVA or Kruskal-Wallis rank test followed by Wilcoxon-Mann-Whitney test for normally and nonnormally distributed continuous variables, respectively. ‡Percentage weight reduced from maximum was calculated from self-report of lifetime maximum weight. §Activity was assessed by self-report via the International Physical Activity Questionnaire (*N* = 20 IGT and *N* = 16 T2D). ‖Subscales of eating behavior were assessed with the Three-Factor Eating Questionnaire Revised 18-item version (TFEQ-R18). Missing data include VAT *N* = 1 (T2D), LDL *N* = 3 (T2D), attempting to lose weight *N* = 2 (NGT), *N* = 1 (IGT). *$P < 0.05$ vs. NGT; †$P < 0.05$ vs. IGT. Significant *P* values are in boldface.

1.2). On average, changes in body composition and glucose over 1 year were minimal (Supplementary Table 3). There was interindividual variability in the magnitude and direction of change over 1 year in measures of glucose tolerance, β-cell function, and insulin sensitivity (Fig. 3*A*–*D*). In models with adjustment for age, baseline MBH T2 relaxation times were unrelated to percentage change in glucose iAUC, disposition index, or glucose sensitivity (Fig. 3*E*–*G*), as were control region values (data not shown). However, a significant negative association was found between MBH T2 relaxation time and change in OGIS (Fig. 3*H*), consistent with 1-year declines in insulin sensitivity among those with longer MBH T2 relaxation times at baseline. Moreover, increases in total body fat tended to be related to baseline MBH T2 relaxation times (β = 0.04%, *P* = 0.07) and gains in VAT were significantly associated (β = 6.2 g, *P* = 0.03). For assessment of the extent to which the association of changes in OGIS with baseline MBH T2 relaxation time was accounted for by intervening changes in total body adiposity, the change in percentage of body fat was added to the age-adjusted model, and it appeared to explain a portion of the variance, as both the β-coefficient and *P* value were reduced after changes in body fat were accounted for (adjusted β = −0.25 to −0.16; *P* = 0.03 to *P* = 0.13).

CONCLUSIONS

The current study provides radiologic evidence that alterations in hypothalamic tissue are present in IGT and T2D and that the magnitude of tissue-level changes parallels progression of glucose dysregulation in obesity. Participants with IGT or T2D had longer mean MBH T2 relaxation times, an MRI-derived marker of gliosis (12,14,26), as compared with those with NGT, despite all groups having the same degree of elevated body fat mass. The findings were limited to the MBH region in which the arcuate nucleus is located, were not present in control regions, and were independent of age, sex, and percent body fat. Moreover, fasting glucose

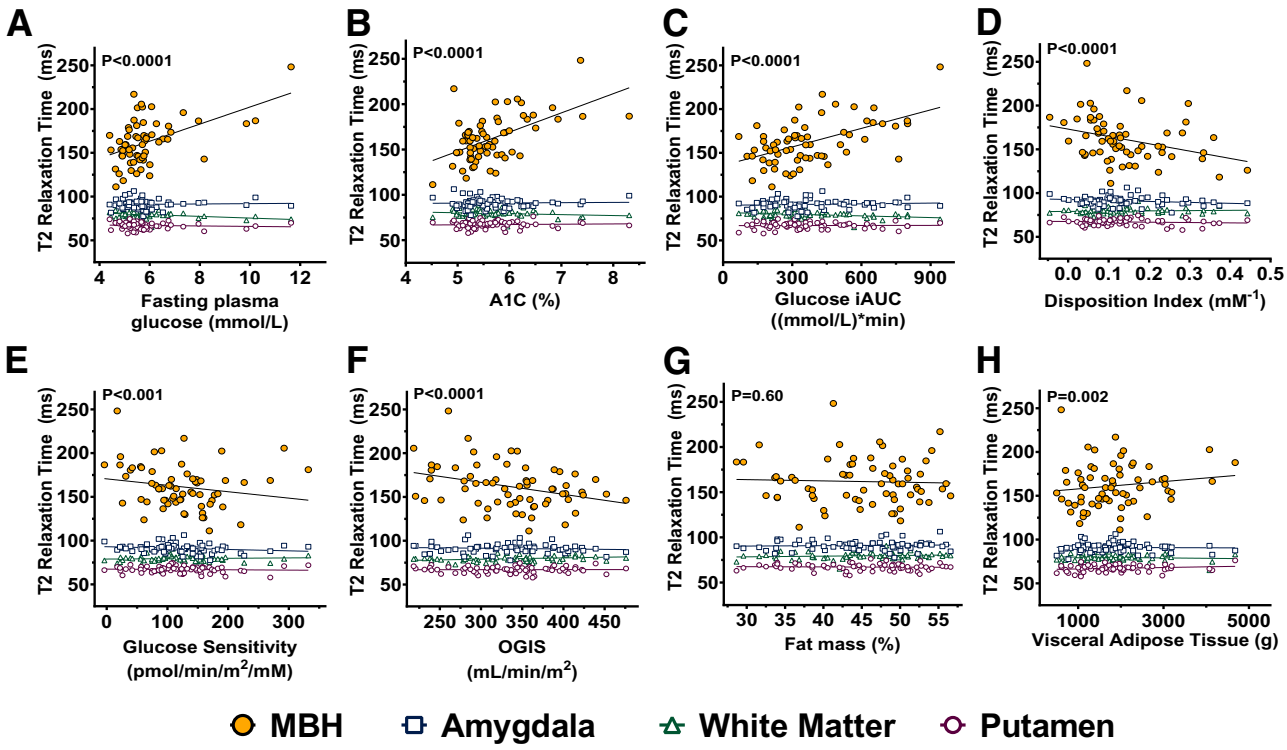

Figure 2—Age-adjusted cross-sectional associations of T2 relaxation time with measures of glycemia, glucose tolerance, β-cell function, insulin sensitivity, and adiposity among all participants, stratified by brain region. Positive linear associations of MBH T2 relaxation time (filled gold circles) were present for fasting plasma glucose (*A*), hemoglobin A_{1c} (*B*), and glucose iAUC (*C*). Negative linear associations were present with MBH T2 relaxation time and the disposition index (insulinogenic index * [1 / fasting insulin]) (*D*), glucose sensitivity (*E*), and OGIS index (*F*). MBH T2 relaxation time was not related to total body fat mass percentage (*G*) but was positively associated with VAT mass (*H*). There were no associations within any control regions (open symbols) for any measure. Generalized estimating equation models included outcome data from all brain regions, an interaction term (predictor * region), and a covariate for age (age-adjusted data shown). *P* values reported on graphs derived from model posttests of linear association for the MBH region. *N* = 67. Missing data include: fasting glucose, glucose iAUC, insulin iAUC, glucose sensitivity, OGIS (*N* = 2), VAT (*N* = 1).

concentrations, glucose excursions during an OGTT, and hemoglobin A_{1c} were positively associated with longer MBH T2 relaxation times, whereas indices of β-cell function and insulin sensitivity declined as MBH T2 relaxation times increased. Several of these relationships persisted when the sample was restricted to participants without T2D, indicating that early metabolic abnormalities including rising hemoglobin A_{1c} concentrations, glucose intolerance, and lower disposition index are related to evidence of gliosis prior to the development of clinically significant elevations in blood glucose. Finally, MBH T2 relaxation times at baseline were related to worsening insulin sensitivity over 1 year of observational follow-up among participants with NGT or IGT. Collectively, the results provide novel evidence that both the degree and progression of metabolic dysregulation in humans are related to structural changes within hypothalamic tissue.

Prior human studies consistently demonstrate hypothalamic tissue alterations consistent with inflammation or gliosis in association with overweight or obesity through diverse methodologies including diffusion MRI (27), immunohistochemistry in postmortem samples (13,18), quantitative water content mapping (19), and quantitative T2 (4,13–17), as used in the current study. While evidence of inflammation in lateral hypothalamus (19) and fornix (19,28) has been observed, most studies focused on the mediobasal region. Given mounting evidence of MBH gliosis in obesity in humans and rodent models with diet-induced obesity, as well as the neuronal and glial cell populations residing in the MBH that control peripheral glucose levels (9,10,29), the current study specifically tested the MBH in relation to metabolic impairments among individuals with obesity. Previous neuroimaging studies of MBH gliosis and insulin resistance provided mixed results (13,14), but the current findings are robust and consistent across multiple measures indicative of insulin resistance.

The current study extends prior work through measurement of insulin sensitivity and β-cell function using a glucose modeling approach (22) that correlates with clamp-derived measures of insulin sensitivity (25). We found not only that insulin sensitivity is lower when the extent of evidence of MBH gliosis is greater but also that the degree of MBH gliosis presages future deterioration in insulin sensitivity. The latter finding was modestly attenuated after changes in body fat were accounted for, suggesting that gains or losses in adiposity explain some, but not all, of this prospective association. Moreover, the oral disposition index, a measure of early β-cell response that predicts future T2D onset (30), was significantly related to MBH T2 relaxation times among people with obesity but no diabetes. In contrast, the association of glucose sensitivity, an assessment of β-cell sensitivity to glucose, with MRI measures did

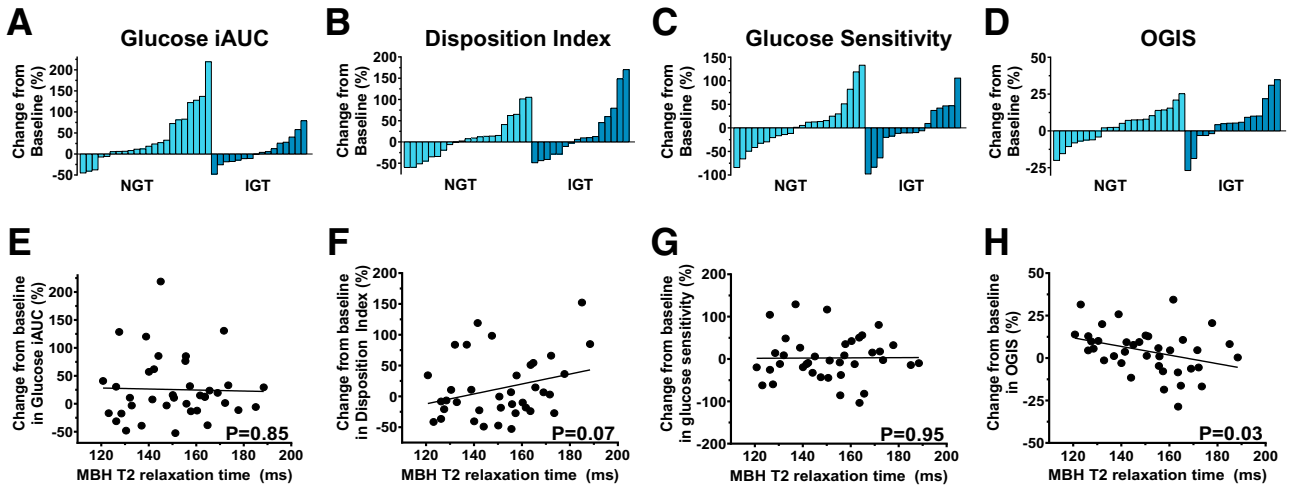

Figure 3—Prospective association of baseline MBH gliosis with 1-year change in response to OGTT among participants with obesity and IGT or NGT at baseline. *A–D*: Waterfall plots depicting individual percentage change from baseline over 1 year in results of a 2-h, 75-g OGTT, with stratification by NGT and IGT at baseline. Age-adjusted linear associations of baseline MBH T2 relaxation time were absent for percentage change from baseline in glucose iAUC (*E*), disposition index (*F*), and glucose sensitivity (*G*), but a negative association was present with OGIS index (*H*). Generalized estimating equation models included outcome data from all brain regions, an interaction term (predictor * region), and a covariate for age (age-adjusted data shown). *P* values reported on graphs derived from model posttests of linear association for the MBH region. *N* = 38.

not persist when participants with T2D were excluded from analyses. It may be that insulin sensitivity and early insulin response are more closely related to the presence and degree of hypothalamic gliosis than β-cell dose-response to glucose, but further study is required. The results also provide novel evidence of relationships between MBH gliosis and fasting glucose concentrations, glucose intolerance, and hemoglobin A_{1c}. Finally, marked elevations in MBH T2 signal were observed in participants with T2D, reaffirming prior research in clinical populations with T2D and metabolic syndrome (15,19). Taken as a whole, these results advance our understanding that not only is hypothalamic gliosis present in obesity but also its severity may have implications for the development of metabolic dysregulation and comorbidities.

The results also suggest that MBH gliosis may be more closely correlated to the degree of metabolic dysregulation than variability in adiposity in adults with obesity. Investigators in prior neuroimaging studies observed positive linear relationships between MRI-derived markers and body adiposity (4,14,17,19,20,27). However, these studies included subjects with BMIs in the normal and overweight ranges. Taken together, available findings suggest that MBH gliosis contributes both to obesity development and, once obesity is established, to progressive metabolic impairment. Consistent with this hypothesis, we found that MBH gliosis positively correlated with visceral fat mass, echoing prior findings (17,19,20) and implicating MBH gliosis in a shift toward deposition of metabolically unhealthy fat.

The quantitative T2 technique used in this study assesses tissue composition as a whole. The cellular mechanisms underlying the findings therefore cannot be verified, but prior literature and preclinical studies provide insight into how disruption of function of specific cell types within the MBH might impact peripheral glucose regulation. First, neuron populations might be reduced as seen in chronic high-fat diet feeding (4), with implications for glucose regulation (29). In humans, one study of the left hypothalamus by MRS saw no evidence of altered neuronal cell counts (13); however, the spatial resolution of this technique is low, and reduced cell populations within specific nuclei or subregions cannot be ruled out. Second, the function of key neuron populations or their neuron-glia interactions might be altered. Moreover, normal processes such as hypothalamic neurogenesis, which is impaired in diet-induced obesity (31), and synaptic plasticity, which is known to be leptin inducible in the arcuate nucleus (32) and is dependent on coresident microglial populations (33), might also be impaired. Finally, glial cells are increasingly recognized as having independent roles in orchestrating the CNS response to energy availability (10) including hypothalamic glucose sensing (8), satiety signaling in the hindbrain (34), and sustained remission of hyperglycemia by injection of fibroblast growth factor 1 (9). In postmortem studies, microglial dystrophy (18) and astrocyte proliferation (14) were present in humans with obesity and longer MBH T2 relaxation times, respectively. These data provide translational evidence that glial cell morphology—at minimum—is altered in the MBH of humans with obesity and has potential negative consequences for glial cells' participation in maintenance of normal peripheral glucose homeostasis. In sum, although human data remain sparse and are limited by the anatomic resolution of in vivo imaging techniques and reliance on postmortem histology, existing data support the relevance of an expanding basic science literature regarding the important role of glial cells and neuron-glia interactions in obesity and T2D pathogenesis.

The current findings were bilateral and robust, in contrast to prior findings that were lateralized to one or the other side of the hypothalamus (4,13). Additional strengths of the study include the clinically meaningful group definitions, matching of the groups for adiposity, and inclusion of prospective analyses. Conclusions are limited by the cross-sectional nature of some analyses and the

relatively smaller sample size available for the longitudinal component. Participants were predominantly female, but the sex distribution was consistent across groups and effects persisted in models with adjustment for sex. Nonetheless, rodent studies have shown sex-related variability; therefore, further studies powered to detect effect modification by sex would be useful. Moreover, we interpret the findings as consistent with hypothalamic gliosis based on prior rodent and postmortem human studies correlating longer MBH T2 relaxation times on a multiecho T2 acquisition with reactive astrocytosis on ex vivo histologic examination (12,14). Despite these and other histopathologic studies associating gliosis with high T2 signal (26,35,36), MRI is an indirect measure. We cannot exclude edema, infection, or tumor as explanations for the findings, although these seem unlikely in this neurologically healthy sample, and we cannot state definitively that findings were within the arcuate. The ventromedial nucleus is in close proximity, and portions could have been sampled within the MBH region of interest. Additionally, we used OGIS to estimate insulin sensitivity, whereas clamps are the gold standard. Finally, 1 year may have been too brief a period of follow-up to detect changes in glucose tolerance or β-cell function.

In conclusion, these translational findings support a role for the CNS in T2D pathogenesis. Specifically, MBH gliosis may represent a shared pathogenic process that contributes to both obesity and impaired glucose homeostasis through its effects on their integrated neurocircuitry (37). Preclinical mechanistic studies will be required to test this hypothesis and resolve areas of uncertainty between overlapping factors such as overnutrition and impaired metabolic function that are difficult to disentangle in human studies. When chronic, gliosis is a form of permanent scarring (38); thus, its long-term clinical implications require additional study. Structural remodeling of the hypothalamus would fit with the clinical presentations of obesity and T2D as chronic conditions that remit but do not resolve with current therapies—with the notable exception of bariatric surgery, which potentially modifies MBH gliosis (15). In rodents, dietary factors trigger hypothalamic inflammation and gliosis (39), theoretically as an adaptive response to short-term overnutrition (6), and reversion to chow diet ameliorates gliosis (11). Further studies to ascertain dietary determinants in humans are needed, as are tests of nutritional strategies to prevent or reverse gliosis. Resolution of these outstanding questions is critical to progress the field toward identifying novel CNS targets for prevention and treatment of T2D.

Acknowledgments. Supplementary Fig. 1 and parts of Fig. 2 were created with BioRender (https://biorender.com).

Funding. This work was supported by American Diabetes Association Innovative Clinical or Translational Science award 1-17-ICTS-085 (to E.A.S.). Additional support was from National Institutes of Health (NIH) awards R01DK089036 (E.A.S.), R01DK117623 (E.A.S.), K24HL144917 (E.A.S.), and T32HL007028 (J.L.R.) and University of Washington Nutrition and Obesity Research Center grant P30DK035816 and Diabetes Research Center grant P30DK017047. K.M.U. is supported by the Veterans Affairs Administration. Some study data were collected and managed using REDCap electronic data capture tools hosted at the University of Washington Institute of Translational Health Sciences, which are supported by NIH National Center for Advancing Translational Sciences award UL1TR002319. The authors acknowledge the University of Pennsylvania Diabetes Research Center (NIH grant DK19525) for measurement of glucose, insulin, and C-peptide.

Duality of Interest. No potential conflicts of interest relevant to this article were reported.

Author Contributions. S.J.M., K.M.U., and E.A.S. conceptualized the study. J.L.R., M.F.W., M.R.B.D.L., and M.H. collected data. J.L.R., S.J.M., S.S., and K.M.U. analyzed data. S.J.M. and E.A.S. performed statistical analyses. J.L.R., S.J.M., K.M.U., and E.A.S. wrote the manuscript. All authors read the manuscript and agreed with its content and conclusions. E.A.S. is the guarantor of this work and, as such, had full access to all the data in the study and takes responsibility for the integrity of the data and the accuracy of the data analysis.

Prior Presentation. Parts of this study were presented in abstract form at the 81st Scientific Sessions of the American Diabetes Association, New Orleans, LA, 25–29 June 2021.

References

1. Myers MG Jr, Affinati AH, Richardson N, Schwartz MW. Central nervous system regulation of organismal energy and glucose homeostasis. Nat Metab 2021;3:737–750
2. Deem JD, Muta K, Scarlett JM, Morton GJ, Schwartz MW. How should we think about the role of the brain in glucose homeostasis and diabetes? Diabetes 2017;66:1758–1765
3. De Souza CT, Araujo EP, Bordin S, et al. Consumption of a fat-rich diet activates a proinflammatory response and induces insulin resistance in the hypothalamus. Endocrinology 2005;146:4192–4199
4. Thaler JP, Yi CX, Schur EA, et al. Obesity is associated with hypothalamic injury in rodents and humans. J Clin Invest 2012;122:153–162
5. Jastroch M, Morin S, Tschöp MH, Yi CX. The hypothalamic neural-glial network and the metabolic syndrome. Best Pract Res Clin Endocrinol Metab 2014;28:661–671
6. Valdearcos M, Xu AW, Koliwad SK. Hypothalamic inflammation in the control of metabolic function. Annu Rev Physiol 2015;77:131–160
7. Morton GJ, Schwartz MW. Leptin and the central nervous system control of glucose metabolism. Physiol Rev 2011;91:389–411
8. García-Cáceres C, Quarta C, Varela L, et al. Astrocytic insulin signaling couples brain glucose uptake with nutrient availability. Cell 2016;166:67–880
9. Bentsen MA, Rausch DM, Mirzadeh Z, et al. Transcriptomic analysis links diverse hypothalamic cell types to fibroblast growth factor 1-induced sustained diabetes remission. Nat Commun 2020;11:4458
10. García-Cáceres C, Balland E, Prevot V, et al. Role of astrocytes, microglia, and tanycytes in brain control of systemic metabolism. Nat Neurosci 2019;22:7–14
11. Berkseth KE, Guyenet SJ, Melhorn SJ, et al. Hypothalamic gliosis associated with high-fat diet feeding is reversible in mice: a combined immunohistochemical and magnetic resonance imaging study. Endocrinology 2014;155:2858–2867
12. Lee D, Thaler JP, Berkseth KE, Melhorn SJ, Schwartz MW, Schur EA. Longer T(2) relaxation time is a marker of hypothalamic gliosis in mice with diet-induced obesity. Am J Physiol Endocrinol Metab 2013;304:E1245–E1250
13. Kreutzer C, Peters S, Schulte DM, et al. Hypothalamic inflammation in human obesity is mediated by environmental and genetic factors. Diabetes 2017;66:2407–2415
14. Schur EA, Melhorn SJ, Oh SK, et al. Radiologic evidence that hypothalamic gliosis is associated with obesity and insulin resistance in humans. Obesity (Silver Spring) 2015;23:2142–2148
15. van de Sande-Lee S, Melhorn SJ, Rachid B, et al. Radiologic evidence that hypothalamic gliosis is improved after bariatric surgery in obese women with type 2 diabetes. Int J Obes 2020;44:178–185
16. Sewaybricker LE, Melhorn SJ, Papantoni A, et al. Pilot multi-site and reproducibility study of hypothalamic gliosis in children. Pediatr Obes 2021;16:e12732
17. Sewaybricker LE, Schur EA, Melhorn SJ, et al. Initial evidence for hypothalamic gliosis in children with obesity by quantitative T2 MRI and implications for blood oxygen-level dependent response to glucose ingestion. Pediatr Obes 2019;14:e12486
18. Baufeld C, Osterloh A, Prokop S, Miller KR, Heppner FL. High-fat diet-induced brain region-specific phenotypic spectrum of CNS resident microglia. Acta Neuropathol 2016;132:361–375
19. Kullmann S, Abbas Z, Machann J, et al. Investigating obesity-associated brain inflammation using quantitative water content mapping. J Neuroendocrinol 2020;32:e12907
20. Berkseth KE, Rubinow KB, Melhorn SJ, et al. Hypothalamic gliosis by MRI and visceral fat mass negatively correlate with plasma testosterone

concentrations in healthy men. Obesity (Silver Spring) 2018;26:1898–1904
21. Baroncini M, Jissendi P, Balland E, et al. MRI atlas of the human hypothalamus. Neuroimage 2012;59:168–180
22. Mari A, Schmitz O, Gastaldelli A, Oestergaard T, Nyholm B, Ferrannini E. Meal and oral glucose tests for assessment of beta-cell function: modeling analysis in normal subjects. Am J Physiol Endocrinol Metab 2002;283:E1159–E1166
23. Mari A, Ferrannini E. Beta-cell function assessment from modelling of oral tests: an effective approach. Diabetes Obes Metab 2008; 10(Suppl. 4):77–87
24. Van Cauter E, Mestrez F, Sturis J, Polonsky KS. Estimation of insulin secretion rates from C-peptide levels. Comparison of individual and standard kinetic parameters for C-peptide clearance. Diabetes 1992;41:368–377
25. Mari A, Pacini G, Murphy E, Ludvik B, Nolan JJ. A model-based method for assessing insulin sensitivity from the oral glucose tolerance test. Diabetes Care 2001;24:539–548
26. Briellmann RS, Kalnins RM, Berkovic SF, Jackson GD. Hippocampal pathology in refractory temporal lobe epilepsy: T2-weighted signal change reflects dentate gliosis. Neurology 2002;58:265–271
27. Thomas K, Beyer F, Lewe G, et al. Higher body mass index is linked to altered hypothalamic microstructure. Sci Rep 2019;9:17373
28. Metzler-Baddeley C, Baddeley RJ, Jones DK, Aggleton JP, O'Sullivan MJ. Individual differences in fornix microstructure and body mass index. PLoS One 2013;8:e59849
29. Parton LE, Ye CP, Coppari R, et al. Glucose sensing by POMC neurons regulates glucose homeostasis and is impaired in obesity. Nature 2007;449:228–232
30. Utzschneider KM, Prigeon RL, Faulenbach MV, et al. Oral disposition index predicts the development of future diabetes above and beyond fasting and 2-h glucose levels. Diabetes Care 2009;32:335–341
31. McNay DE, Briançon N, Kokoeva MV, Maratos-Flier E, Flier JS. Remodeling of the arcuate nucleus energy-balance circuit is inhibited in obese mice. J Clin Invest 2012; 122:142–152
32. Pinto S, Roseberry AG, Liu H, et al. Rapid rewiring of arcuate nucleus feeding circuits by leptin. Science 2004;304:110–115
33. Kettenmann H, Kirchhoff F, Verkhratsky A. Microglia: new roles for the synaptic stripper. Neuron 2013;77:10–18
34. Reiner DJ, Mietlicki-Baase EG, McGrath LE, et al. Astrocytes regulate GLP-1 receptor-mediated effects on energy balance. J Neurosci 2016;36:3531–3540
35. Chung YL, Williams A, Ritchie D, et al. Conflicting MRI signals from gliosis and neuronal vacuolation in prion diseases. Neuroreport 1999;10:3471–3477
36. Jackson GD, Williams SR, Weller RO, et al. Vigabatrin-induced lesions in the rat brain demonstrated by quantitative magnetic resonance imaging. Epilepsy Res 1994;18: 57–66
37. Alonge KM, D'Alessio DA, Schwartz MW. Brain control of blood glucose levels: implications for the pathogenesis of type 2 diabetes. Diabetologia 2021;64:5–14
38. Sofroniew MV. Molecular dissection of reactive astrogliosis and glial scar formation. Trends Neurosci 2009;32:638–647
39. Moraes JC, Coope A, Morari J, et al. High-fat diet induces apoptosis of hypothalamic neurons. PLoS One 2009;4:e5045